Research Article

Drug Testing and Analysis

Received: 17 June 2010 Revised: 9 August 2010 Accepted: 10 August 2010 Published online in Wiley Online Library: 28 October 2010

(www.drugtestinganalysis.com) DOI 10.1002/dta.178

Experimental and spectroscopic studies of charge transfer reaction between sulfasalazine antibiotic drug with different types of acceptors

Moamen S. Refat,[a,b]* Sabry A. El-Korashy,[c] Ibrahim M. El-Deen[a] and Shaima M. El-Sayed[b]

The charge-transfer (CT) interactions between the electron donor sulfasalazine (SS) and the acceptors 2,3-dichloro-5,6-dicyano-1,4-benzoquinone (DDQ), *p*-chloranil (CHL), picric acid (PA) and iodine have been studied spectrophotometrically in $CHCl_3$ or CH_3OH solutions. The formed solid CT complexes were also isolated and characterized through infrared, ^{1}H-NMR, mass spectra as well as elemental and thermal analysis. The CT complexes were discussed in terms of formation constant (K_{CT}), molar extinction coefficient (ε_{CT}), standard free energy (ΔG°), oscillator strength (f), transition dipole moment (μ), resonance energy (R_N) and ionization potential (I_D). The stoichiometry of these complexes was found to be 1 : 1 molar ratio and having the formulae [(SS)(DDQ)], [(SS)(CHL)], [(SS)(PA)] and $[(SS)_2I]^+ \cdot I_3^-$, respectively. The charge transfer interaction was successfully applied to the determination of SS drug using mentioned σ and π-acceptors also, the results obtained herein are satisfactory for estimation of SS compound in the pharmaceutical form.

Keywords: sulfasalazine (SS); charge-transfer complexes; TG/DTG; IR; acceptor

Introduction

Sulfasalazine (SS) (Formula 1) is a sulfa drug, a derivative of Mesalazine (5-aminosalicylic acid abbreviated as 5-ASA), used primarily as an anti-inflammatory agent in the treatment of inflammatory bowel disease as well as for rheumatoid arthritis.[1–4]

Charge-transfer (CT) complexation is an important phenomenon in biochemical and bioelectrochemical energy transfer process.[5] CT interactions between electron donors and acceptors are generally associated with the formation of intensely coloured CT complexes which absorb radiation in the visible region.[6] Molecular complexation and structural recognition are important processes in biological systems; for example, drug action, enzyme catalysis, and ion transfers through lipophilic membranes all involve complexation.[7]

Mulliken suggested that the formation of molecular complexes from two aromatic molecules can arise from the transfer of an electron from a π–molecular orbital of a Lewis base to vacant π- molecular orbital of a Lewis acid, with resonance between this dative structure and the no-band structure stabilizing the complex.[8] Mulliken also noted the possibility of complex formation through the donation of an electron from a non- bonding molecular orbital in a Lewis base to a vacant π-orbital of an acceptor (n-π)[9] with resonance stabilization of the combination.

The CT complexation is an important technique that is cheaper, simpler, and more efficient than the methods of drug determination described in the literature.[10–13] The CT reactions of SS with I_2, DDQ, CHL and PA have not yet been reported in the literature; therefore the aim of the present study was to investigate these reactions.

Results of elemental analysis for all the SS CT complexes are listed in Table 1. It can be seen that values found are in agreement with the calculated values, and the composition of the CT complexes are matched with the molar ratios presented from the photometric titration occurring between SS and acceptors (σ- and π- acceptor). All of the complexes are insoluble in water and alcohol, but easily soluble in dimethyl formamide (DMF) and dimethylsulfoxide (DMSO).

Experimental

Preparation of SS/acceptor charge-transfer complexes (Acceptor = I_2, DDQ, CHL and PA)

SS, ($C_{18}H_{14}N_4O_5S$) was of analytical reagent grade (Merck reagent).

*[**(SS)**]-iodine CT complex*

The solid CT complex of SS with iodine was prepared by mixing (398.39 mg, 1.0 mmol) of the donor in chloroform (10 ml). A

* *Correspondence to: Dr. Moamen S. Refat, Department of Chemistry, Faculty of Science, Port Said 42111, Port Said University, Egypt. E-mail: msrefat@yahoo.com*

a *Department of Chemistry, Faculty of Science, Port Said 42111, Port Said University, Egypt*

b *Department of Chemistry, Faculty of Science, Taif University, 888 Taif, Kingdom Saudi Arabia.*

c *Department of Chemistry, Faculty of Science, Ismalia, Suez Canal University, Ismalia, Egypt*

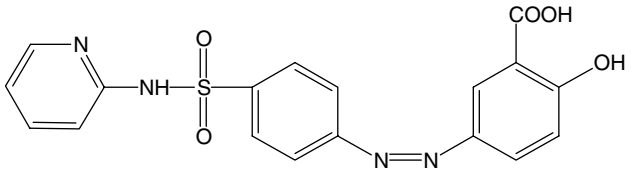

Formula 1. Sulfasalazine (SS).

solution of iodine was added (253.81 mg, 1.0 mmol) in the same solvent and continuously stirred for about 30 min at room temperature. A brown precipitate solution appeared and was allowed to evaporate slowly at room temperature. A brown solid complex was formed, washed several times with small amounts of chloroform, and dried under vacuum over anhydrous calcium chloride; the empirical formula of the complex $[(SS)_2]I^+.I_3^-$ is $C_{36}H_{28}N_8O_{10}S_2I_4$ with molecular weight 1104.40 g/mol.

[(SS)]/DDQ, CHL and PA CT complexes

The solid CT complexes of SS with π-acceptors like (DDQ, CHL, and PA) were prepared by mixing 1 mmol of the donor in 10 ml chloroform with 1 mmol of each acceptor in the same solvent with constant stirring for about 30 min. The solutions were allowed to evaporate slowly at room temperature. The resultant complexes in the solid state were filtered and washed several times with small amounts of solvent, and dried under vacuum over anhydrous calcium chloride. The CT complexes [(SS)(DDQ)] (dark red crystals) formed with empirical formula $C_{26}H_{14}N_6SCl_2O_7$ with molecular weight 625.40 g/mol, [(SS)(CHL)] (orange crystals) formed with empirical formula as $C_{24}H_{14}N_4SCl_4O_7$ with molecular weight 644.27 g/mol and [(SS)(PA)] (red crystals) formed with empirical formula $C_{24}H_{17}N_7SO_{12}$ with molecular weight 627.50 g/mol.

Instrumentation and physical measurements

Electronic spectra

The electronic spectra of the donors, acceptors, and the resulted CT complexes were recorded in the region of 200–800 nm by using a Jenway 6405 Spectrophotometer with quartz cells, 1.0 cm path in length.

Infrared spectra

IR measurements (KBr discs) of the solid donors, acceptor, and CT complexes were carried out on a Bruker FT-IR spectrophotometer (400–4000 cm^{-1}).

^{1}H-NMR spectra

^{1}H-NMR spectra were obtained on a Varian Gemini 200 MHz spectrometer. ^{1}H-NMR data are expressed in parts per million (ppm), referenced internally to the residual proton impurity in DMSO (d_6) solvent and the reported of chemical shift, (m = multiplet, s = singlet and br = broad).

Mass spectra

The compositions of the complexes were confirmed from mass spectra at 70 eV by using AEI MS 30 mass spectrometer.

Thermal analysis

The thermal analysis (TGA/DTG) was carried under nitrogen atmosphere with a heating rate of 10 C/min using a Shimadzu TGA-50H thermal analyzer.

Results and Discussion

Electronic absorption spectrum of SS/iodine, SS/DDQ, SS/CHL and SS/PA systems

The electronic spectra of the iodine, DDQ, CHL, and PA of SS charge-transfer complexes were measured in $CHCl_3$ or MeOH solvents. In the case of $CHCl_3$ or MeOH solvents, the CT complexes are formed by adding X ml of 5.0×10^{-4} M (iodine, DDQ, CHL or PA) (X = 0.25, 0.50, 0.75, 1.00, 1.50, 2.00, 2.50 and 3.00 ml) to 1.00 ml of 5.0×10^{-4} M SS. The volume of the mixtures in each case was completed to 10 ml with the respective solvent. The concentration of SS in the reaction mixture was kept fixed at 0.50×10^{-4} M in the $CHCl_3$ or MeOH solvents, while the concentration of iodine, DDQ, CHL, or PA was varied over the range of 0.125×10^{-4} M to 1.500×10^{-4} M for SS/I_2, SS/DDQ, SS/CHL or SS/PA systems in $CHCl_3$ or MeOH solvents. These concentrations produce SS : acceptor (I_2, DDQ, CHL, and PA) ratios extending along the range from 1 : 0.25 to 1 : 3.00. The electronic absorption spectra of the 1 : 1 ratios in $CHCl_3$ or MeOH together with the reactants (I_2, DDQ, CHL, PA and SS are shown in Figures 1A–1D.

The spectra reveal the characterization of the real absorption bands which are not present in the spectra of the free reactants; iodine, DDQ, CHL, PA, and SS. These bands are assigned at (360 and 288 nm), (537, 410 and 360 nm), 310 nm and (420 and 360 nm) due to the CT complexes formed in the reaction of SS with I_2, DDQ, CHL, and PA, respectively, in the chloroform for iodine system and in methanol solvent in the case of DDQ, CHL, and PA. Tables 2A–2D give the values of the absorbances obtained from photometric titrations based on the distinguished absorption bands around 360 and 288 nm; 537, 410, and 360 nm; 310 nm; and 420 and 360 nm. Photometric titration curves based on these characterized absorption bands are given in Figures 2A–2D.

Table 1. Elemental analysis CHN and physical parameters data of the CT complexes formed in the reaction of the SS with iodine, DDQ, CHL and PA

		C%		H%		N%		Physical data	
Complexes	Mwt	Found	Calc.	Found	Calc.	Found	Calc.	Λm (μs)	mp (°C)
$[(SS)_2]I^+.I_3^-$	1104.4	38.94	39.10	2.52	2.54	9.98	10.10	65	64
[(SS)(DDQ)]	625.4	49.43	49.90	2.21	2.24	13.21	13.40	30	112
[(SS)(CHL)]	644.27	44.54	44.70	2.09	2.17	8.43	8.69	33	109
[SS)(PA)]	627.5	45.67	45.90	2.11	2.71	15.44	15.60	37	135

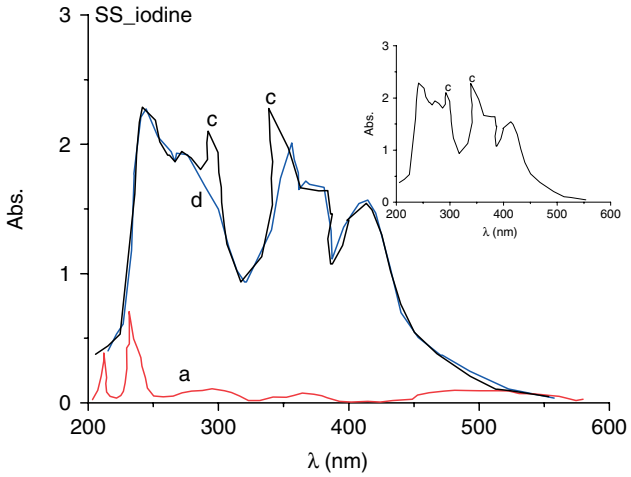

Figure 1A . Electronic absorption spectra of; SS-iodine reaction in $CHCl_3$, where (d) = donor (1.0×10^{-4} M), (a) = acceptor (1.0×10^{-4} M) and (c) = CT complex.

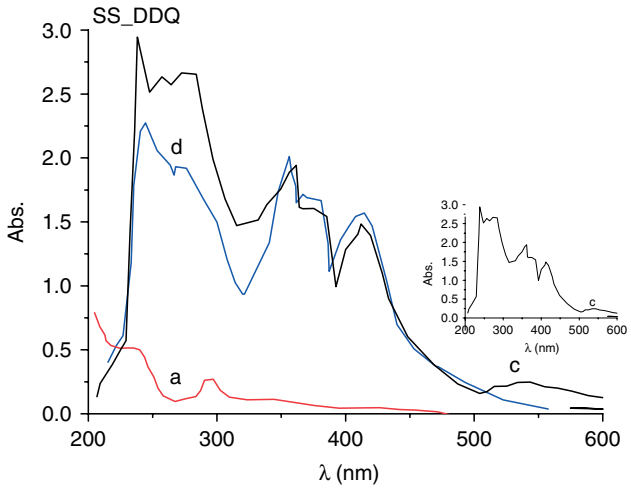

Figure 1B . Electronic absorption spectra of; SS-DDQ reaction in MeOH, where (d) = donor (1.0×10^{-4} M), (a) = acceptor (1.0×10^{-4} M) and (c) = CT complex.

These photometric titration curves were obtained according to known methods[14] by the plot of the absorbance against the X ml added of the iodine σ-acceptor or DDQ, CHL, and PA as π-acceptors. The equivalence points shown in these curves clearly indicate that the formed CT complexes between SS and iodine, DDQ, CHL or PA are 1 : 1. The formation of 1 : 1 complex was strongly supported by elemental analysis, mid infrared, ^{1}HNMR, and mass spectra, as well as thermal analysis TG-DTG.

However, the appearance of the two absorption bands around ≈360 and ≈290 nm are well known[15–17] to be characteristic for the formation of the tri-iodide ion (I_3^-). Accordingly, the formed complex was formulated as $[(SS)_2]I^+.I_3^-$.

It was of interest to observe that the solvent has a pronounced effect on the spectral intensities of the formed $[(SS)_2]I^+.I_3^-$, [(SS)(DDQ)], [(SS)(CHL)] and [(SS)(PA)] complexes. The 1 : 1 modified Benesi-Hildebrand equation[18] was used in the calculations.

$$\frac{C_a^o C_d^o l}{A} = \frac{1}{K\varepsilon} + \frac{C_a^o + C_d^o}{\varepsilon} \quad (1)$$

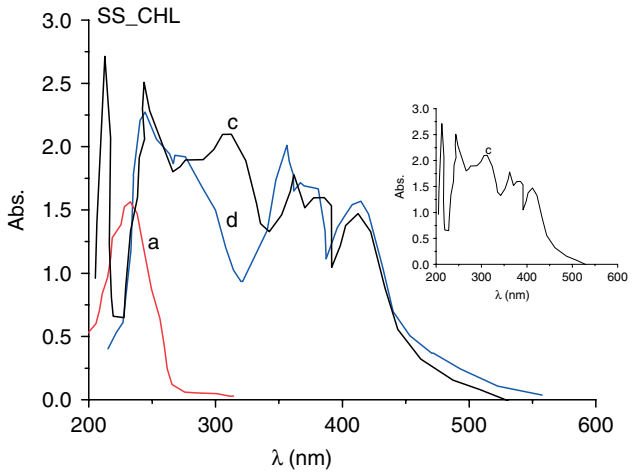

Figure 1C . Electronic absorption spectra of; SS-CHL reaction in MeOH, where (d) = donor (1.0×10^{-4} M), (a) = acceptor (1.0×10^{-4} M) and (c) = CT complex.

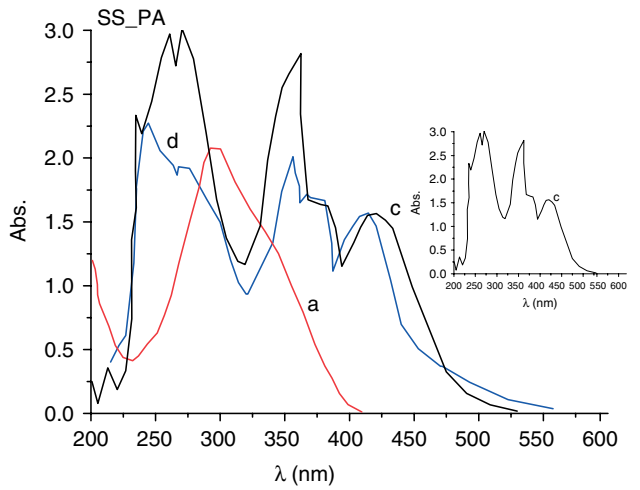

Figure 1D . Electronic absorption spectra of; SS-PA reaction in MeOH, where (d) = donor (1.0×10^{-4} M), (a) = acceptor (1.0×10^{-4} M) and (c) = CT complex.

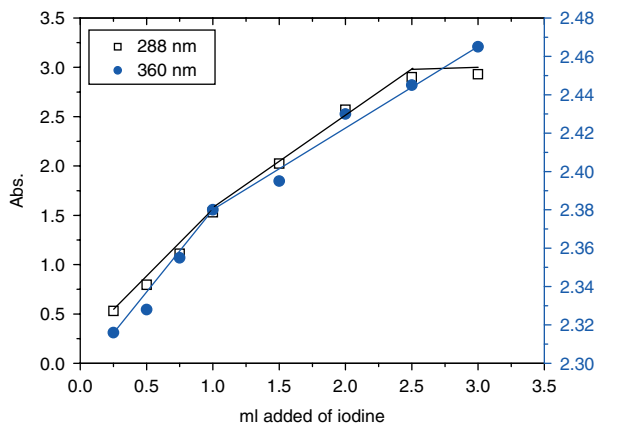

Figure 2A . Photometric titration curve for the SS-I_2 system in $CHCl_3$ at 288 and 360 nm.

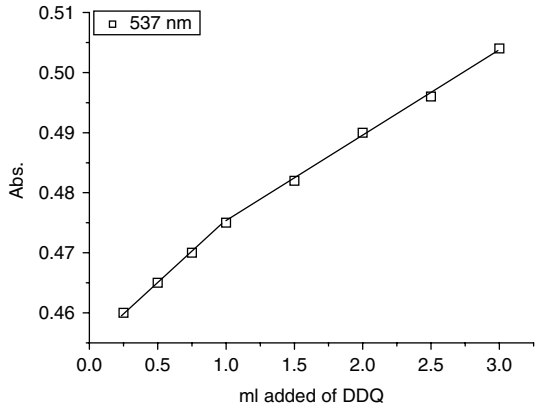

Figure 2B . Photometric titration curve for the SS-DDQ system in MeOH at 537 nm.

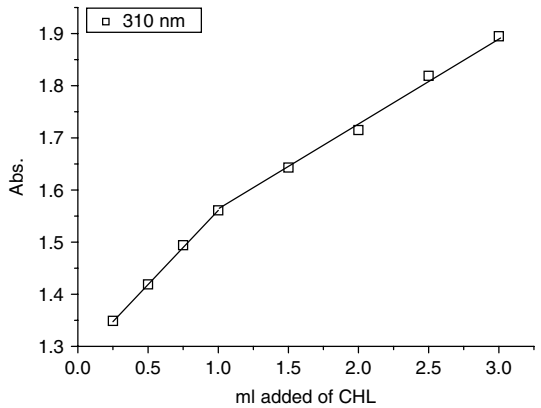

Figure 2C . Photometric titration curve for the SS-CHL system in MeOH at 310 nm.

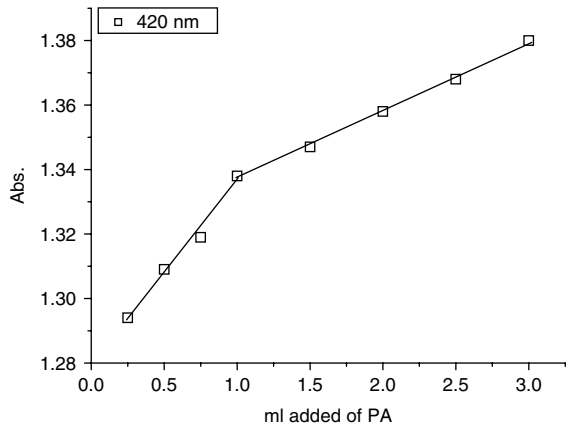

Figure 2D . Photometric titration curve for the SS-PA system in MeOH at 420 nm.

Where C_a^o and C_d^o are the initial concentrations of the acceptors (I_2, DDQ, CHL, or PA) and the donor SS, respectively, K is a formation constant, ε is a molar extinction coefficient, and A is the absorbance of the definite bands around 360 and 288 nm; 537, 410, and 360 nm; 310 nm; and 420 and 360 nm. The data obtained C_d^o of SS, C_a^o of I_2, DDQ, CHL or PA; $C_a^o + C_d^o$; and C_a^o. C_d^o/A in $CHCl_3$ or MeOH solvents are summarized and given in Tables 3A–3D.

Table 2. The electronic absorptions spectral data for SS-iodine, SS-DDQ, SS-CHL and SS-PA CT complexes in $CHCl_3$ or MeOH solvents
1 ml SS(5×10^{-4} M) + X ml iodine(5×10^{-4} M) + Y ml solvent = 10 ml($CHCl_3$ or MeOH)

X ml of iodine	(SS : Iodine) ratio	Absorbance 288 nm	Absorbance 360 nm
0.25	1 : 0.25	0.530	2.316
0.50	1 : 0.50	0.795	2.328
0.75	1 : 0.75	1.111	2.355
1.00	1 : 1.00	1.530	2.380
1.50	1 : 1.50	2.024	2.395
2.00	1 : 2.00	2.570	2.430
2.50	1 : 2.50	2.900	2.445
3.00	1 : 3.00	2.930	2.465

X ml of DDQ	(SS : DDQ) ratio	Absorbance 537 nm
0.25	1 : 0.25	0.460
0.50	1 : 0.50	0.465
0.75	1 : 0.75	0.470
1.00	1 : 1.00	0.475
1.50	1 : 1.50	0.482
2.00	1 : 2.00	0.490
2.50	1 : 2.50	0.496
3.00	1 : 3.00	0.504

X ml of CHL	(SS : CHL) ratio	Absorbance 310 nm
0.25	1 : 0.25	1.349
0.50	1 : 0.50	1.419
0.75	1 : 0.75	1.494
1.00	1 : 1.00	1.561
1.50	1 : 1.50	1.643
2.00	1 : 2.00	1.715
2.50	1 : 2.50	1.819
3.00	1 : 3.00	1.895

X ml of PA	(SS : PA) ratio	Absorbance 420 nm
0.25	1 : 0.25	1.294
0.50	1 : 0.50	1.309
0.75	1 : 0.75	1.319
1.00	1 : 1.00	1.338
1.50	1 : 1.50	1.347
2.00	1 : 2.00	1.358
2.50	1 : 2.50	1.368
3.00	1 : 3.00	1.380

When the $C_a^o.C_d^o$/A values for each solvent ($CHCl_3$ or MeOH) are plotted against the corresponding $C_a^o + C_d^o$ values, straight lines were obtained with a slope of $1/\varepsilon$ and intercept of $1/k\varepsilon$ as shown in Figures 3A–3D. The oscillator strength f was obtained from the approximate formula given in Equation (2)[19]

$$f = (4.319 \times 10^{-9})\varepsilon_{max}.\nu_{1/2} \quad (2)$$

where $\nu_{1/2}$ is the band-width for half-intensity in cm^{-1}. The oscillator strength values together with the corresponding

Table 3. The values C_d^o, C_a^o, $C_d^o + C_a^o$ and $C_d^o.C_a^o/A$, for the SS-iodine, SS-DDQ, SS-CHL and SS-PA systems in $CHCl_3$ or MeOH solvents

SS: Iodine Ratio	$C_d^o \times 10^{-4}$	$C_a^o \times 10^{-4}$	$(C_d^o + C_a^o) \times 10^{-6}$	$(C_d^o.C_a^o) \times 10^{-8}$	$(C_d^o.C_a^o/A) \times 10^{-10}$ 288 nm	360 nm
1 : 0.25	0.5	0.125	62.50	0.0625	0.118	0.0270
1 : 0.50	0.5	0.250	75.00	0.1250	0.157	0.0537
1 : 0.75	0.5	0.375	87.50	0.1875	0.169	0.0796
1 : 1.00	0.5	0.500	100.0	0.2500	0.163	0.1050
1 : 1.50	0.5	0.750	125.0	0.3750	0.185	0.1570
1 : 2.00	0.5	1.000	150.0	0.5000	0.195	0.2060
1 : 2.50	0.5	1.250	175.0	0.6250	0.216	0.2560
1 : 3.00	0.5	1.500	200.0	0.7500	0.256	0.2840
SS: DDQ ratio	$C_d^o \times 10^{-4}$	$C_a^o \times 10^{-4}$	$(C_d^o + C_a^o) \times 10^{-6}$	$(C_d^o.C_a^o) \times 10^{-8}$	$(C_d^o.C_a^o/A) \times 10^{-10}$ 537 nm	
1 : 0.25	0.5	0.125	62.50	0.0625	0.136	
1 : 0.50	0.5	0.250	75.00	0.1250	0.269	
1 : 0.75	0.5	0.375	87.50	0.1875	0.399	
1 : 1.00	0.5	0.500	100.0	0.2500	0.526	
1 : 1.50	0.5	0.750	125.0	0.3750	0.778	
1 : 2.00	0.5	1.000	150.0	0.5000	1.020	
1 : 2.50	0.5	1.250	175.0	0.6250	1.260	
1 : 3.00	0.5	1.500	200.0	0.7500	1.490	
SS: CHL ratio	$C_d^o \times 10^{-4}$	$C_a^o \times 10^{-4}$	$(C_d^o + C_a^o) \times 10^{-6}$	$(C_d^o.C_a^o) \times 10^{-8}$	$(C_d^o.C_a^o/A) \times 10^{-10}$ 310 nm	
1 : 0.25	0.5	0.125	62.50	0.0625	0.0463	
1 : 0.50	0.5	0.250	75.00	0.1250	0.0881	
1 : 0.75	0.5	0.375	87.50	0.1875	0.1260	
1 : 1.00	0.5	0.500	100.0	0.2500	0.1600	
1 : 1.50	0.5	0.750	125.0	0.3750	0.2280	
1 : 2.00	0.5	1.000	150.0	0.5000	0.2920	
1 : 2.50	0.5	1.250	175.0	0.6250	0.3440	
1 : 3.00	0.5	1.500	200.0	0.7500	0.3960	
SS: PA ratio	$C_d^o \times 10^{-4}$	$C_a^o \times 10^{-4}$	$(C_d^o + C_a^o) \times 10^{-6}$	$(C_d^o.C_a^o) \times 10^{-8}$	$(C_d^o.C_a^o/A) \times 10^{-10}$ 420 nm	
1 : 0.25	0.5	0.125	62.50	0.0625	0.0483	
1 : 0.50	0.5	0.250	75.00	0.1250	0.0955	
1 : 0.75	0.5	0.375	87.50	0.1875	0.1420	
1 : 1.00	0.5	0.500	100.0	0.2500	0.1870	
1 : 1.50	0.5	0.750	125.0	0.3750	0.2780	
1 : 2.00	0.5	1.000	150.0	0.5000	0.3680	
1 : 2.50	0.5	1.250	175.0	0.6250	0.4570	
1 : 3.00	0.5	1.500	200.0	0.7500	0.5430	

dielectric constants, *D*, of the solvent used are given in Table 4. The trend of the values in this table reveals two facts:

1. The $[(SS)_2]I^+.I_3^-$, [(SS)(DDQ)], [(SS)(CHL)] and [(SS)(PA)] shows high values of both the equilibrium constant (*K*) and the extinction coefficient (ε). This high value of *K* reflects the high stability of the SS complexes as a result of the expected high donation of the SS, while the high value of ε concerning SS/iodine CT complex agrees quite well with the existence of tri-iodide ion, I_3^-, which is known to have a high absorptivity value.[15–17]
2. The values of the oscillator strength, *f*, increase with the increasing in the dielectric constant (*D*) of the solvent. This result could be explained on the basis of competitive solvent interactions with the acceptors.[20]

The general mechanism for the formation of $[(SS)_2]I^+.I_3^-$ complex is proposed as follows:

$$2SS + I_2 \rightarrow [SS]_2I^+.I^-$$
$$[SS]_2I^+.I^- + I_2 \rightarrow [(SS)_2]I^+.I_3^-$$

The formation of $[SS]_2I^+.I^-$ reaction intermediate is analogous to the well-known species $[(donor)I]^+.I^-$ formed in the reaction of iodine with many donors.[21,22]

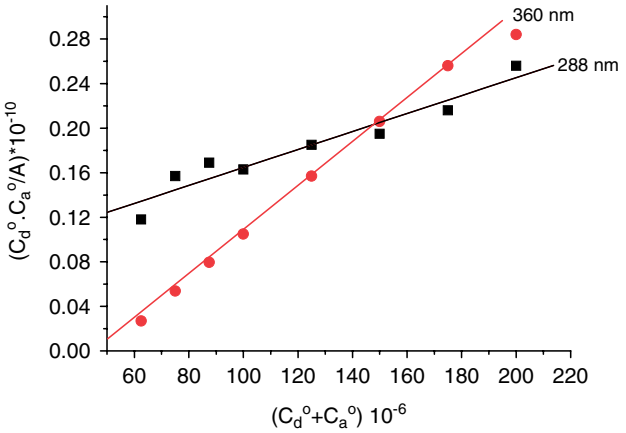

Figure 3A . The plot of ($C_d^\circ + C_a^\circ$) values against ($C_d^\circ.C_a^\circ/A$) values for the SS-iodine system in $CHCl_3$ at 360 and 288 nm.

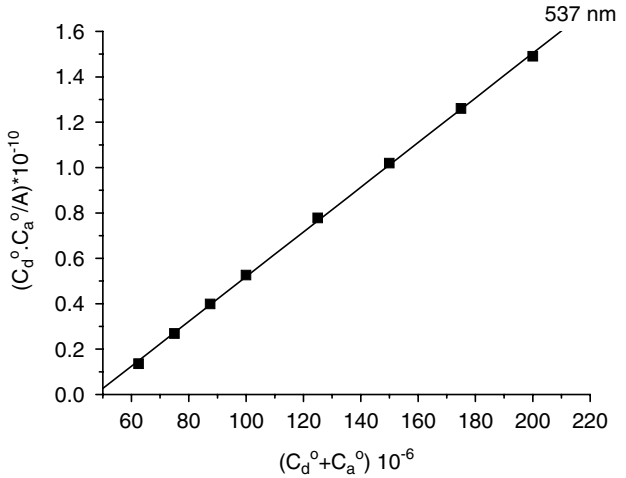

Figure 3B . The plot of ($C_d^\circ + C_a^\circ$) values against ($C_d^\circ.C_a^\circ/A$) values for the SS-DDQ system in MeOH at 537 nm.

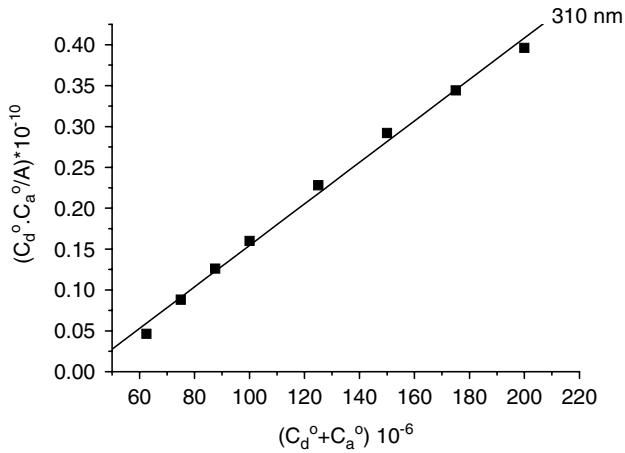

Figure 3C . The plot of ($C_d^\circ + C_a^\circ$) values against ($C_d^\circ.C_a^\circ/A$) values for the SS-CHL system in MeOH at 310 nm.

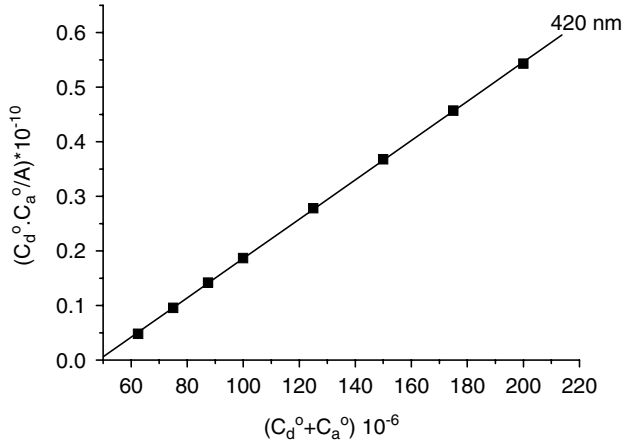

Figure 3D . The plot of ($C_d^\circ + C_a^\circ$) values against ($C_d^\circ.C_a^\circ/A$) values for the SS-PA system in MeOH at 420 nm.

The transition dipole moment (μ) of the SS CT complexes (Table 4) have been calculated from Equation (3)[23]

$$\mu = 0.0958[\varepsilon_{max}\nu_{1/2}/\nu_{max}]^{1/2} \quad (3)$$

where $\nu_{1/2}$ is the bandwidth at half-maximum of absorbance, ε_{max} and ν_{max} are the extinction coefficient and wavenumber at maximum absorption peak of the CT complexes, respectively.

The ionization potential (I_p) of the free SS donor was determined from the CT energies of the CT band of its complexes with iodine by using the following relationships:[24]

$$E_{CT}(ev) = I_p - 5.2 + 1.5/(I_p - 5.2) \quad (4a)$$

The ionization potentials of the donor (I_D) in the CT complexes of SS/DDQ, SS/CHL or SS/PA are calculated using empirical equation derived by Aloisi and Piganatro.[25]

$$I_D(ev) = 5.76 + 1.53 \times 10^{-4}\ \nu_{CT} \quad (4b)$$

Where E_{CT} is the energy of the CT of the SS complexes, the energy of the π-σ^*, n-σ^*, π-π^* or n-π^* interaction (E_{CT}) is calculated using Equation (5)[23]

$$E_{CT}(ev) = (h\nu_{CT}) = 1243.667/\lambda_{CT}(nm) \quad (5)$$

where, λ_{CT} is the wavelength of the complexation band.

Determination of resonance energy (R_N), from Briegleb and Czekalla[26] theoretically derived the relation given in Equation (6)

$$\varepsilon_{max}(l.mol^{-1}.cm^{-1}) = 7.7 \times 10^{-4}/[h\nu_{CT}/[R_N] - 3.5] \quad (6)$$

where ε_{max} is the molar extinction coefficient of the complex at the maximum CT absorption, ν_{CT} is the frequency of the CT peak, and R_N is the resonance energy of the complex in the ground state, which obviously is a contributing factor to the stability constant of the complex (a ground state property). The values of R_N for the iodine, DDQ, CHL, and PA complexes under study are given in Table 4. The standard free energy changes of complexation (ΔG°) were calculated from the association constants by Equation (7)[27]

$$\Delta G^\circ = -2.303\ RT\ \log K_{CT} \quad (7)$$

where ΔG° is the free energy change of the complexes (KJ mol^{-1}), R is the gas constant (8.314 J mol^{-1} K), T is the temperature in

Table 4. Spectrophotometric results of the SS CT complex with iodine, DDQ, CHL and PA in $CHCl_3$ or MeOH solvents at 25 °C

$[(SS)_2]I^+.I_3^-$									
λ_{max} (nm)	E_{CT} (eV)	K (l.mol^{-1})	ε_{max} (l.mol^{-1}.cm^{-1})	$f \times 10^3$	$\mu \times 10^3$	I_p	D	R_N	ΔG° (25 °C) KJmol^{-1}
360	3.45	4.65×10^4	427×10^4	4.61	0.594	10.00	4.70	0.995	26 600
[(SS)(DDQ)]									
λ_{max} (nm)	E_{CT} (eV)	K (l.mol^{-1})	ε_{max} (l.mol^{-1}.cm^{-1})	$f \times 10^3$	$\mu \times 10^3$	I_p	D	R_N	ΔG° (25 °C) KJmol^{-1}
537	2.32	1.96×10^4	104×10^4	0.499	0.239	8.82	33	0.969	24 500
[(SS)(CHL)]									
λ_{max} (nm)	E_{CT} (eV)	K (l.mol^{-1})	ε_{max} (l.mol^{-1}.cm^{-1})	$f \times 10^3$	$\mu \times 10^3$	I_p	D	R_N	ΔG° (25 °C) KJmol^{-1}
310	4.01	1.9×10^4	426×10^4	2.19	0.380	10.70	33	0.993	30 100
[(SS)(PA)]									
λ_{max} (nm)	E_{CT} (eV)	K (l.mol^{-1})	ε_{max} (l.mol^{-1}.cm^{-1})	$f \times 10^3$	$\mu \times 10^3$	I_p	D	R_N	ΔG° (25 °C) KJmol^{-1}
420	2.96	1.99×10^4	281×10^4	1.76	0.396	9.40	33	0.991	24 500

Kelvin degrees (273 + °C), and K_{CT} is the association constant of the complexes (l mol^{-1}) in different solvents at room temperature. The values thus calculated are represented in Table 4.

Infrared spectra of the SS/iodine, SS/DDQ, SS/CHL and SS/PA solid complexes

The mid-infrared spectra of SS and the formed CT complex, $[(SS)_2]I^+.I_3^-$, were recorded from KBr discs. These spectra are shown in Figures 4A and 4B, respectively. The spectral bands are assigned to their vibrational modes and given in Table 5. As expected, the bands characteristic for the SS unit in $[(SS)_2]I^+.I_3^-$ CT complex are shown with changes in band intensities and frequency values. In the 4500–3000 cm^{-1} region, no changes in frequencies or intestines occurs; this means that CT complexation did not take place during the –OH, –COOH or –NH groups. On the other hand, the characteristic bands of pyridine moiety are more susceptible to influence; this is evident when examining the region 1500–1350 cm^{-1}. Also, all bands within this region are hypochromically affected, decreasing the intensity of ν(C═C) and ν(C═N) stretched vibrations in the case of iodine complex rather than SS in free feature.

Such changes clearly indicate that the lone pair of electrons on nitrogen atom of pyridine nucleus in SS donor is participated in the complexation process with iodine. The absence of a few bands at around 2600–2400 cm^{-1} due to hydrogen bonding in the SS/iodine complex[28] is strongly interpretive of the mode of interaction between SS and iodine through lone pair of electron of : N (pyridine) not *via* forming hydrogen bond between –OH, –COOH or –NH groups in SS donor and iodine acceptor. The $[(SS)_2]I^+.I_3^-$ CT complex (Formula 2) reported the iodine molecule is attached to a lone pair of electrons on the nitrogen atom of pyridine ring and N···I—N angle is 180°.

The IR spectra of the SS 1 : 1 CT complexes formed from the interaction of the SS and the π-acceptor with the general formula, [(SS)(π-acceptor)] are shown in Figure 4. The full interpretations of the infrared bands are summarized in Table 6.

The IR spectral bands of the free donor, SS, and π-acceptors (DDQ, CHL, and PA) with the corresponding existed in the IR spectra of the isolated solid CT complexes clearly indicate that the characteristic bands of SS show some shift in the frequencies (Table 6), as well as some change in their band's intensities.

The IR spectrum of the CT complex of DDQ with SS contains some of the differences that will lead us to know the type and location of the CT complexation between the SS donor and the acceptor, which can be summarized as follows:

4000–3000 cm^{-1} region: This area includes some of the vibrations for the –OH, –NH and –COOH groups, and these values appear at 3424–3100 cm^{-1}. The stretching vibration of -OH group has not changed, which confirms that it has not participated in the complexation.

3000–2000 cm^{-1} region: This area includes the values of ν(CH) of the aromatic rings and the characteristic peak of the ν(C≡N) band of the free acceptor which is weak and decreases upon CT complexation and changes in the electronic environment.

2000–1000 cm^{-1} region: This region is important in interpretation of the results; it was found by the shift to lower wavenumber of the distinctive value of the C═O groups of –COOH (donor) and C═O of (DDQ) which appear in the starting materials at 1670 cm^{-1} and in SS/DDQ complex at 1640 cm^{-1}. DDQ is deprived of any acidic centres, thus it may be concluded that the molecular complex is formed through π-π^* and/or n-π^* charge migration from HOMO of the donor to LUMO of the acceptor.[28] The interpretation of IR spectra strongly supported that the CT interaction in case of SS/DDQ complex occurs through n-π^* transition. The mechanism of the reaction produced by the proposed method depends on the formation of an intermolecular hydrogen bonding between donor-acceptor (D-A) complex through the interaction between -COOH moiety of the SS drug as n-electron donor and C═O of DDQ as π-acceptor. The hydrogen bonding confirmed by the presence of some characteristic new bands at 3099 cm^{-1} with strong broad intensity and also many of weak to very weak bands within the 2400–2700 cm^{-1} region. The association of D-A complex was promoted by the high ionizing power of the solvent methanol where complete electron transfer from the donor to the acceptor moiety takes place (Formula 3).

The infrared spectrum of [(SS)(CHL)] CT complex has a new band at 3099 cm^{-1} which assigned to intermolecular hydrogen

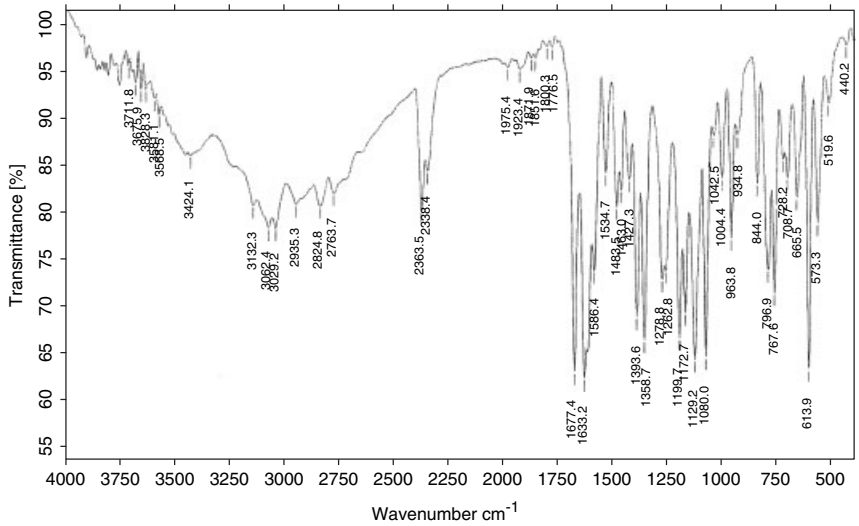

Figure 4A . Infrared spectra of SS.

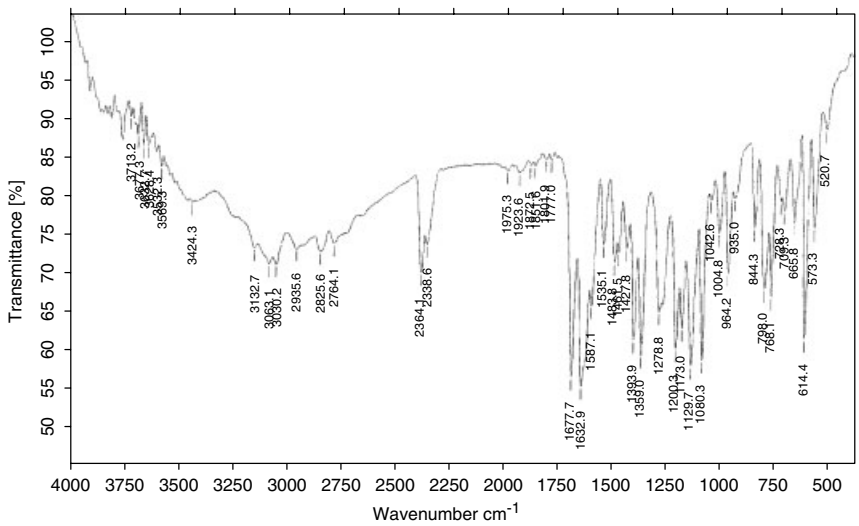

Figure 4B . Infrared spectra of $[(SS)_2]I^+.I_3^-$ CT complex.

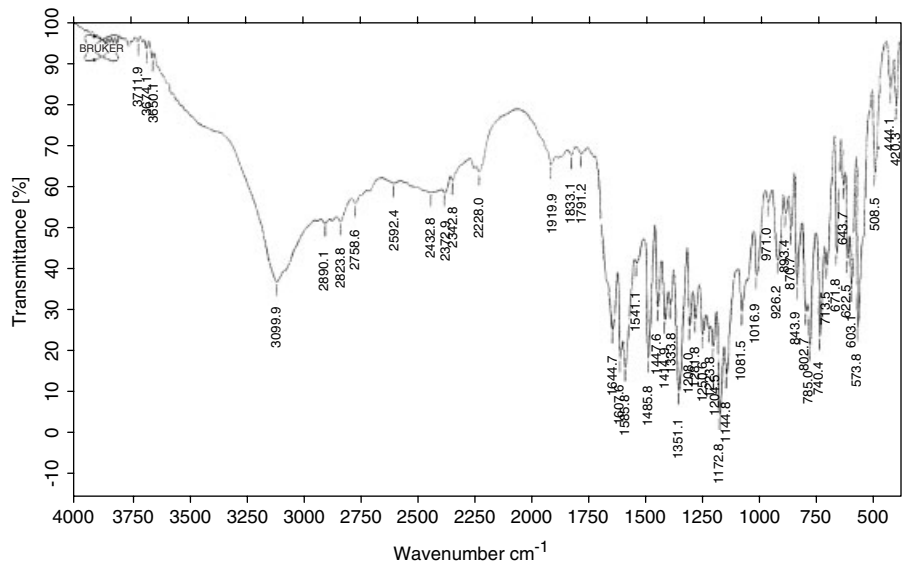

Figure 4C . Infrared spectra of [(SS)(DDQ)] CT complex.

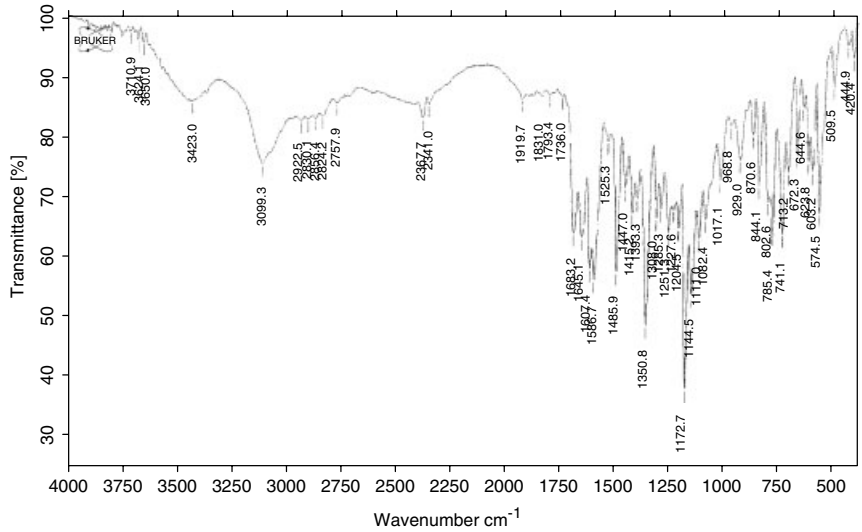

Figure 4D . Infrared spectra of [(SS)(CHL)] CT complex.

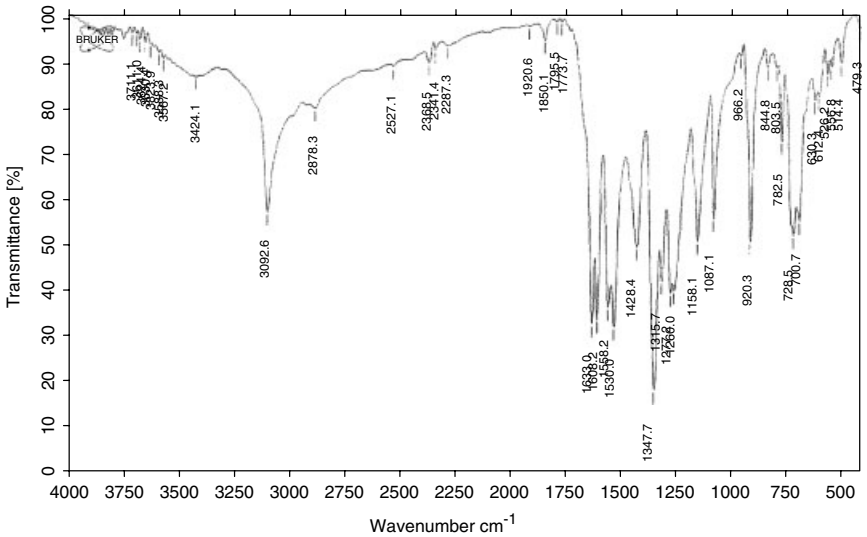

Figure 4E . Infrared spectra of [(SS)(PA)] CT complex.

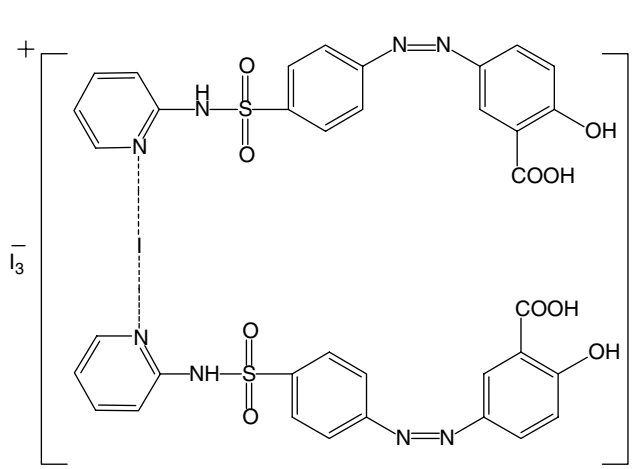

Formula 2. $[(SS)_2]I^+.I_3^-$ CT complex.

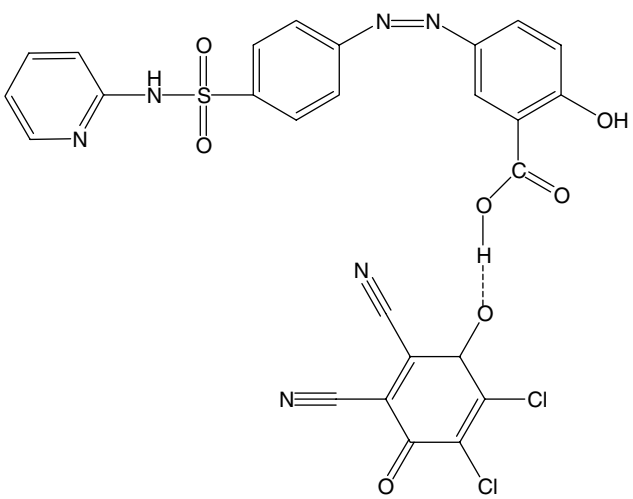

Formula 3. Structure of the [(SS)(DDQ)] CT complex.

Table 5. Infrared frequencies[a] (cm^{-1}) and tentative assignments for SS donor and $[(SS)_2]I^+.I_3^-$ complex

SS	$[(SS)_2]I^+.I_3^-$	Assignments[b]
3424 s,br	3424 s,br	ν(N-H); -NH_2 and –NH
3132 vw	3132 vw	ν(O-H); -OH
3062 vw	3063 vw	ν(C-H); aromatic
3029 vw	3030 vw	
2935 mw	2935 w	ν_s(C-H) + ν_{as}(C-H); CH_3
2824 mw	2825 w	
2763 w	2764 vw	
–	–	Hydrogen bonding
1677 vs	1677 vs	ν(C═O); -COOH
1633 vs	1632 vs	ν(C═C)
1586 sh	1587 sh	δ_{def}(N-H)
		Ring breathing bands
		Pyridine moiety
1534 s	1535 ms	C-H deformation
1483 m	1483 vw	Pyridine moiety
1463 w	1427 w	
1427 m		
1393 s	1393 s	ν(C-C)
1358 vs	1359 s	ν(C-N)
1267 s	1278 s	ν(C-O)
1199 s	1200 s	$\nu(SO_2)$
1172 ms	1173 s	
1129 vs	1129 s	
1080 vs	1080 s	
	1042 vw	
1004 m	1004 ms	(C-H) bend
964 s	964 s	δ_{rock}; NH
844 s	935 vw	
796 s	844 ms	
767 s	798 s	
	768 s	
	728 vw	
708 m	709 w	CH_2 Rock
655 ms	665 ms	Skeletal vibrations
613 vs	614 vs	
573 s	573 s	CNC deformation
519 m	520 w	
440 vw		

[a] : s = strong, w = weak, m = medium, sh = shoulder, v = very, br = broad.
[b] : ν, stretching; δ, bending.

bond occurs between hydrogen atom of –COOH with one of C═O group of CHL acceptor. This bond accompanied by red shift with decreasing in the intensities of all major bands.

The vibration frequencies of the (ν(N–H) + ν(O–H)) and ($\nu_{as}(SO_2) + \nu_s(SO_2)$) groups for SS observed at 3423 cm^{-1} and 1350 + 1172 cm^{-1} did not shift but the intensities were affected; this means that –NH, -OH and SO_2 groups do not share in the CT complexation. The stretching vibrations of ν(C═O) absorption band in case of free CHL and C═O of –COOH of SS donor appeared at 1685 and 1677 cm^{-1}, respectively; under complexation this band is present at 1683 cm^{-1} with decreasing intensity of the band. The bands associated with ν(C-Cl) vibration which appeared at 903 and 709 cm^{-1} in the free CHL were shifted to the lower wavenumbers at 870 and 672 cm^{-1} and decreased the intensity of

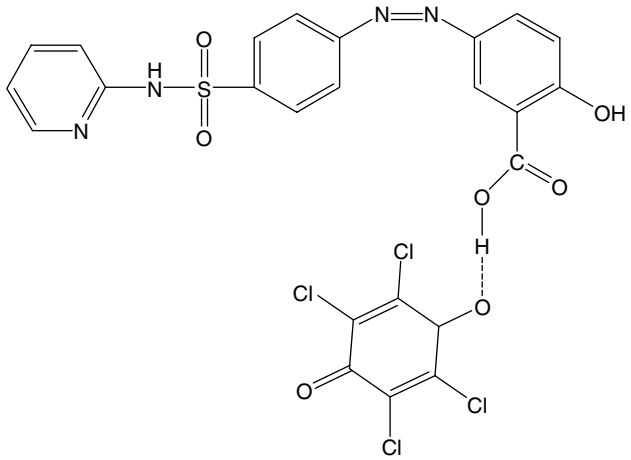

Formula 4. Structure of the [(SS)(CHL)] CT complex.

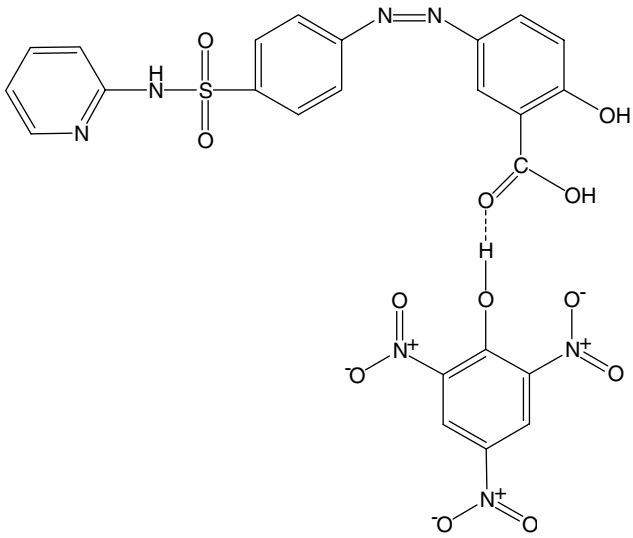

Formula 5. Structure of the [(SS)(PA)] CT complex.

the characteristic peaks; these results are due to the increase in the electron density around CHL moiety. Formula 4 gives a perception of the structure of the [(SS)(CHL)] complex.

The infrared spectrum of the SS/PA CT complex is characterized by a sharp strong singlet band appearing at 3092 cm^{-1}, which does not exist in the spectra of the free SS donor and PA acceptor. This band is attributed to the stretching vibration of the intermolecular hydrogen bond.[28] This result caused the formation of the hydrogen bond between protons of picric acid and oxygen of the (C═O) of the COOH group of the donor. This suggestion is further supported by the absence of the stretching vibration of C═O of the –COOH group of SS donor due to the intermolecular hydrogen bond forming. The shift occurs in the IR bands of the PA acceptor moiety to lower wavenumbers and also of the donor moiety due to D-A charge transfer interaction, $D_{HOMO} \rightarrow D_{LUMO}$ transition.[29] Accordingly, the hydrogen bonding between the SS donor and the PA acceptor can be formulated as Formula 5.

^{1}H-NMR spectrum of [(SS)(PA)] complex

The ^{1}HNMR spectra present the persuasive confirmation of the complexation pathway. Thus, the ^{1}HNMR spectra of both SS free

Table 6. Infrared frequencies[a] (cm^{-1}) and tentative assignments for DDQ, CHL, PA, [(SS)(DDQ)], [(SS)(CHL)] and [(SS)(PA)] CT complexes

			[(SS)(acceptor)] CT complexes			
DDQ	CHL	PA	DDQ	CHL	PA	Assignments[b]
3325 w	3354 ms	3416 br	3425 br	3423 s,br	3421 br	$\nu_{(O-H)}$
3218 br		3103 ms	3099 s,br	3099 s,br	3092 s	ν(N-H); –NH ν(C-H); aromatic
–	–	2980 sh	2890 vw	2922 vw	2878 vw	$\nu_{s(C-H)} + \nu_{as(C-H)}$
		2872 w	2823 vw	2890 vw		
			2758 vw	2856 vw		
				2824 vw		
–	–	–	2592 w	2500–2700 vw	2500–2700 vw	Hydrogen bonding
2250 vw	–	–	2228 m,br	–	–	$\nu_{(C\equiv N)}$; DDQ
2231 ms						
1673 vs	1685 vs	1861 ms	1644 ms	1683 s	1633 vs	ν(C=O); -COOH
		1632 vs	1607 ms	1645 s		$\nu(NO_2)$; PA
		1608 vs				$\nu_{(C=O)} + \nu_{(C=N)}$
		1529 vs				Pyridine moiety
–	–	–	1585 ms	1607 sh	1608 vs	δ_{def}(N-H)
						Ring breathing bands
1552 vs	1567 vs	1432 s	1541 vw	1588 s	1558 sh	$\nu_{(C=C)}$
1451 s	1487 w		1485 s	1522 vw	1530 vs	C-H deformation
			1447 ms	1485 s	1428 s	Pyridine moiety
			1414 m	1447 ms		
				1415 ms		
1358 w	1316 w	1343 ms	1393 w	1393 w	1347 vs	$\nu_{(C-C)} + \nu_{(C-N)}$
1267 s	1257 s	1312 w	1250 w	1350 vs	1315 s	ν(C-O) + $\nu(SO_2)$
1172 vs	1232 s	1263 w	1223 w	1285 mw	1277 s	CH, in-plane bend
1072 w	1210 vw	1150 ms	1204 w	1251 ms	1260 s	
	1110 vs	1086 s	1172 s	1204 ms	1158 s	
			1144 m	1172 vs	1087 s	
			1081 ms	1144 ms		
1010 vw	903 s	917 vs	1016 ms	1017 ms	966 vw	δ_{rock}; NH
893 s	750 s	829 w	971 vw	968 vw	920 vs	
800 vs	709 s	781 s	926 mw	929 ms	844 vw	$\nu_{(C-Cl)}$
720 s		732 s	893 w	870 ms	803 vw	
			870 ms	844 ms	782 s	
				785 ms	728 s	
615 ms	–	703 s	713 w	672 ms	700 s	skeletal vibration
527 vw		652 sh	671 ms		630 vw	CH bend
457 ms	471 mw	522 ms	573 vs	574 s	575 vw	CH out of plane bend
432 mw			508 s	509 ms	556 vw	Skeletal vibration
			444 m	445 w	514 w	CNC def.
			420 m	420 w	429 vw	δ(ONO); PA

[a] : s = strong, w = weak, m = medium, sh = shoulder, v = very, br = broad.
[b] : ν, stretching; δ, bending.

donor and [(SS)(PA)] CT complex in DMSO at room temperature were measured and are given in Figure 5. The chemical shifts (ppm) of proton NMR for the detected peaks are assigned and listed in Table 7. Comparison with those of spectrum of the free SS indicate that SS ligand interacted through the carboxylic COOH group.[1] HNMR spectra of SS/PA CT complex were assigned and the data were obtained in good agreement with the suggested complexation which occurs through the carboxylic group by absence of the distinguished signal of proton which exists in the free ligand at about δ = 11.00 ppm. The different chemical environments of the aromatic protons within the range of 6.00–8.00 ppm are present with decreasing intensities.

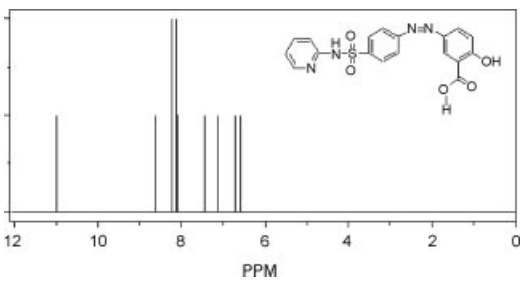

Figure 5A . [1]H-NMR spectrum of SS.

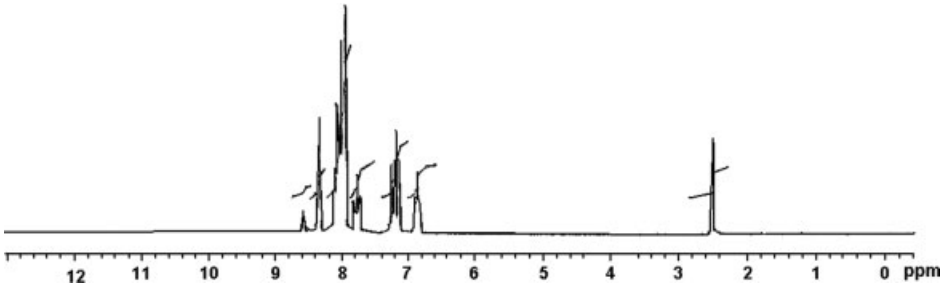

Figure 5B . [1]H-NMR spectrum of [(SS)(PA)] CT complex.

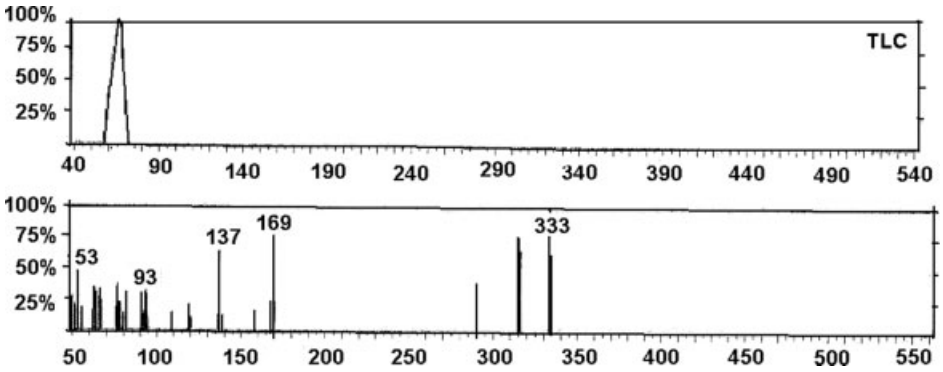

Figure 6. Mass spectrum of [(SS)(DDQ)] CT complex.

Table 7. [1]HNMR data of SS and SS/PA compounds

Compounds	H; OH SS	H; aromatic rings SS+PA	1H; -NH	1H; -COOH
SS	6.854	7.00–8.50	10.90	11.00
[(SS)(PA)]	6.898	7.199–8.591	10.95	–

The signal distinguish to H proton of OH acceptor at ~12 ppm disappeared due to intermolecular hydrogen bond from acceptor to donor.

Mass spectrum of [(SS)(DDQ)] complex

Mass spectrum (Figure 6) of SS/DDQ CT complex shows a series of peaks at *m/z* (%) = 333(100%), 315(75%), 290(38%), 169(91%), 157(15%), 137(64%), 120(11%), 110(21%), 93(31%), 81(30%), 78(36%) and 53(47%) amu corresponding to various fragments. The intensities of these peaks gave an idea of the stabilities of the fragments. Differences in fragmentation were caused by the nature of the attached acceptors through the

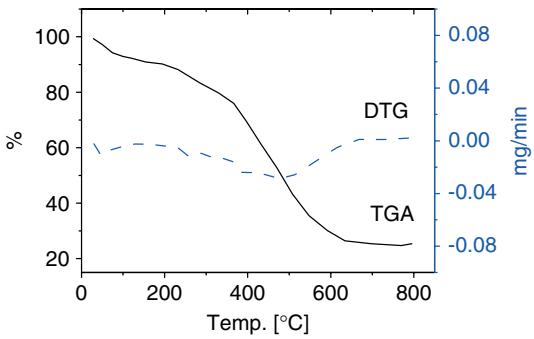

Figure 7B . TG-DTG curve of $[(SS)_2]I^+.I_3^-$ CT complex.

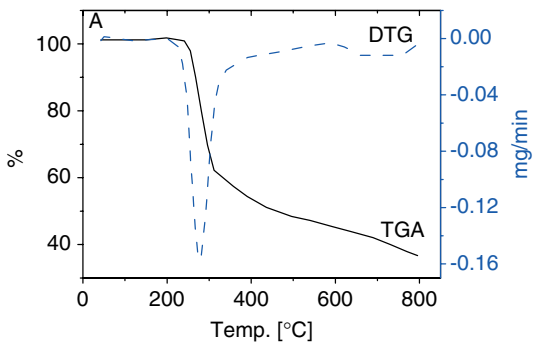

Figure 7A . TG-DTG curve of SS free ligand.

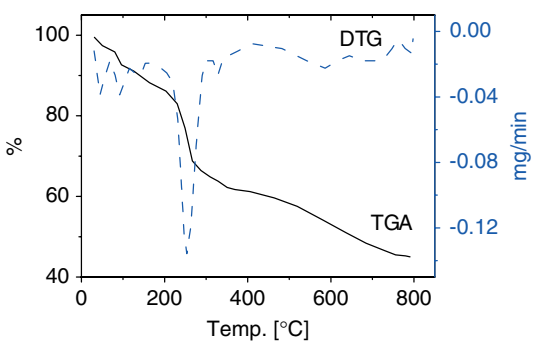

Figure 7C . TG-DTG curve of [(SS)(DDQ)] CT complex.

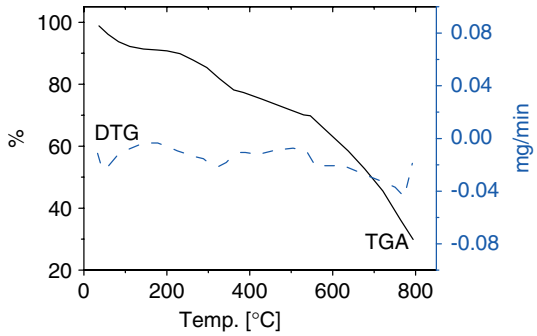

Figure 7D . TG-DTG curve of [(SS)(CHL)] CT complex.

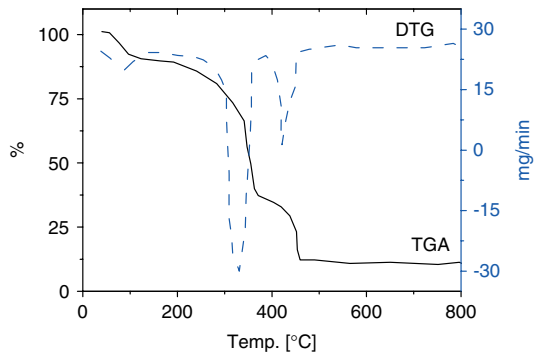

Figure 7E . TG-DTG curve of [(SS)(PA)] CT complex.

intermolecular hydrogen bond between SS and DDQ, while the base peak existed at $m/z = 333$.

Thermal analysis studies

The SS ligand melts at 279 °C with simultaneous decomposition (Figure 7). The thermal decomposition of SS occurs completely in one sharp step which was observed at 279 °C corresponding to the loss of $C_4H_6N_4SO_3$ and $C_2H_8O_2$ (organic moiety) representing a weight loss of obs = 47.20%, calc = 47.69; and obs = 16.50%, calc = 16.00, respectively, then leaving residual carbon as final fragment.

$[(SS)_2]I^+.I_3^-$ CT complex was thermally decomposed in four successive decomposition steps within the temperature range of 25–800 °C. The first-to-fourth decomposition steps occur at 25–130 °C, 130–350, 350–450, and 450–800 °C with maximum peaks at 60, 271, 400, and 565 °C, respectively. The total percentage of weight loss observed ~73.00% matched with the calculated weight loss 72.80% and corresponds to the loss of $C_{11}H_{28}N_8S2O_{10}I_4$ (organic moiety). The decomposition of the iodine complex ended with a carbon as a final residue.

The TG curve of [(SS)(DDQ)] CT complex indicates that the mass change begins at ~100 °C and continuous up to 800 °C. The first-to-third mass loss corresponds to the liberation of $C_{10}H_{14}N_6SCl_2O_7$ molecules (obs = 69.00%, calc = 69.30%). The DTG profile shows three endothermic peaks at 100, 250 and 350 °C. The final decomposition of the SS/DDQ complex is a residual carbon atom.

[(SS)(CHL)] CT complex is thermally stable and decomposed in five medium weak successive decomposition steps interfering within the temperature range 30–800 °C. The first-to-five decomposition steps (obs = 69.76%, calc = 70.20) within the temperature range 30–800 °C at maximum peaks DTG_{max} = 65, 330, 500, 575, and 770 °C, respectively, may be attributed to the liberation of $C_8H_{17}N_7SO_{12}$ organic moiety. The decomposition of the CHL complex molecule ended with final residual carbon atoms.

The CT complex [(SS)(PA)] is thermally stable up to 35 °C and undergoes decomposition beyond this temperature. There are three maxima decomposition steps at DTG_{max} = 90, 310, and 455 °C with mass loss within the temperature range 35–800 °C which corresponds to elimination of $C_{16}H_{17}N_7SO_{12}$ organic moiety (obs = 85.00%, calc = 84.70%). The final residual according the decomposition steps is carbon atoms.

Kinetic studies

In recent years there has been increasing interest in determining the rate-dependent parameters of solid-state non-isothermal decomposition reactions by analysis of TG curves. Several equations[30–32] have been proposed as means of analyzing a TG curve and obtaining values for kinetic parameters.

Two major different methods are used for the evaluation of kinetic parameters.

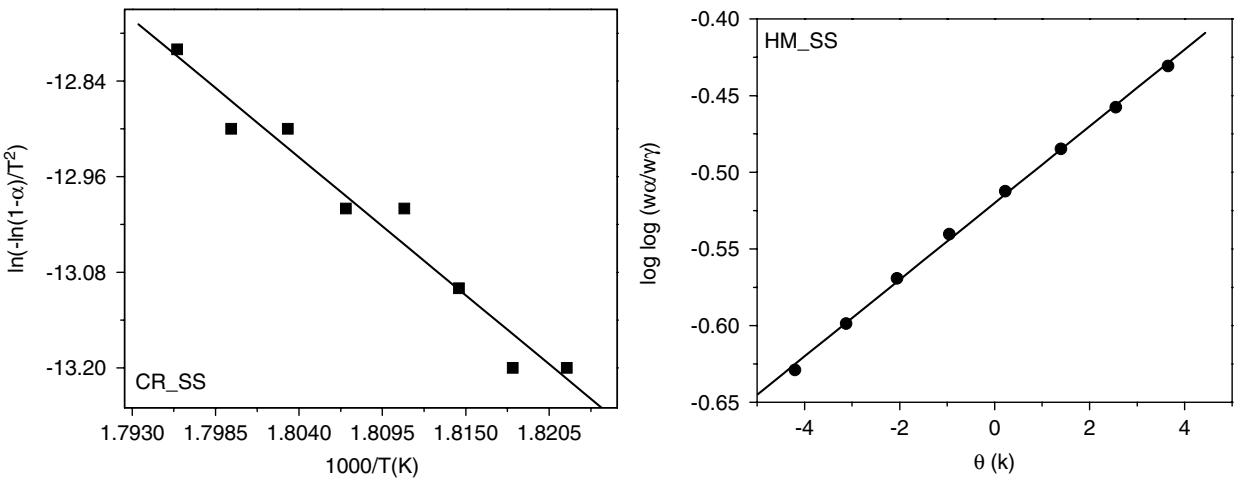

Figure 8A . Kinetic curves of the decomposition steps of SS compound.

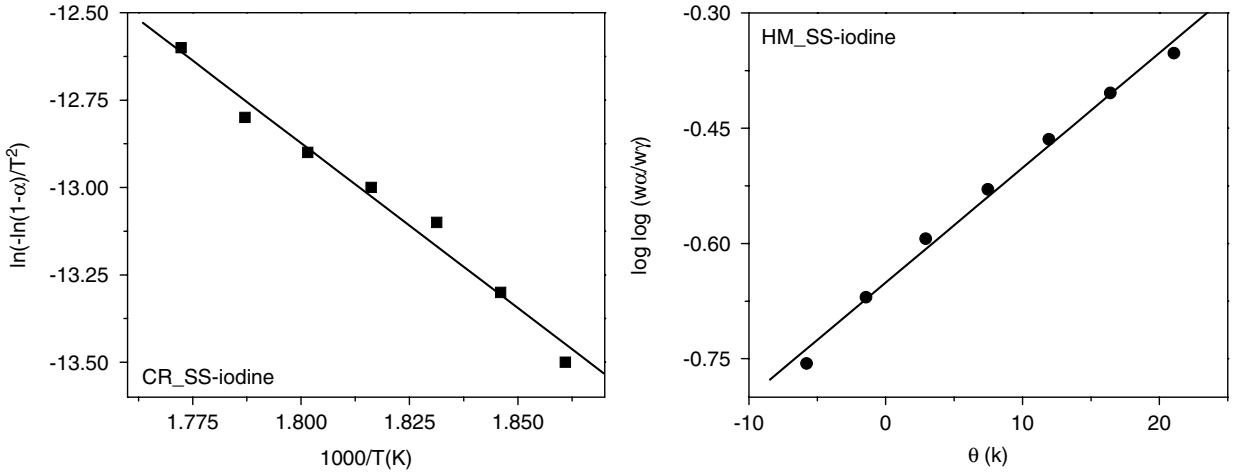

Figure 8B . Kinetic curves of the decomposition steps of SS/iodine CT complex.

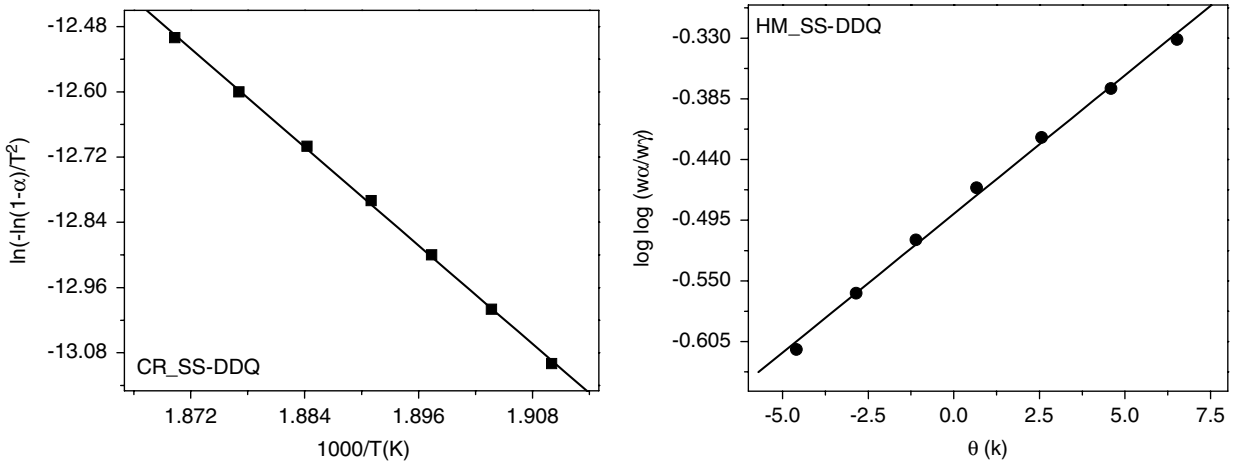

Figure 8C . Kinetic curves of the decomposition steps of SS/DDQ CT complex.

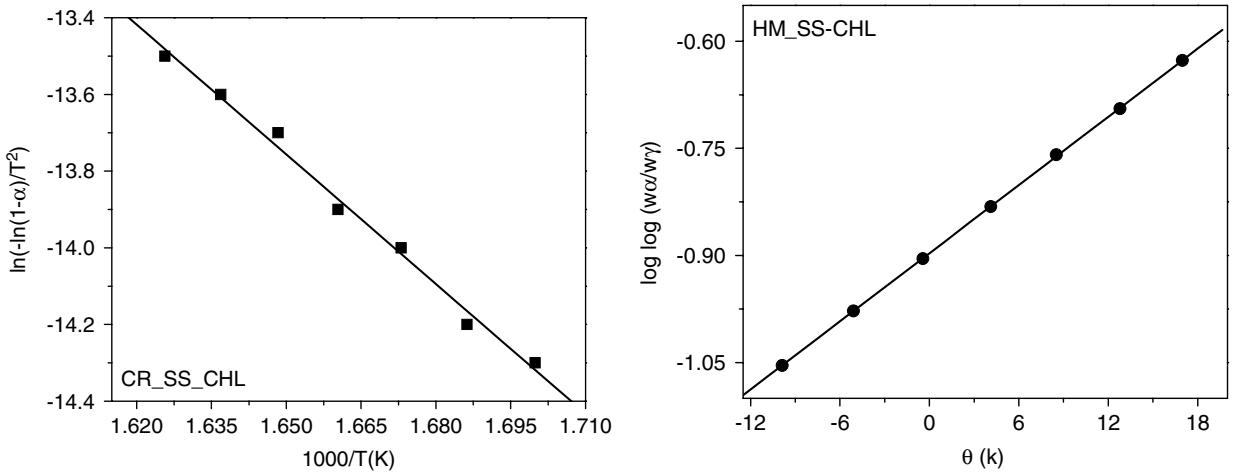

Figure 8D . Kinetic curves of the decomposition steps of SS/CHL CT complex.

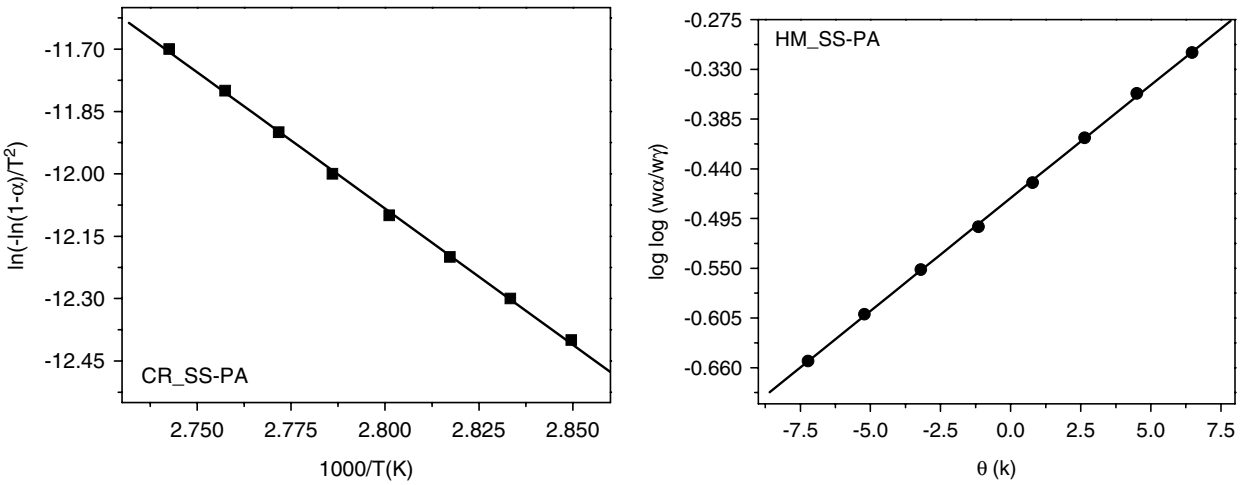

Figure 8E . Kinetic curves of the decomposition steps of SS/PA CT complex.

Table 8. Kinetic parameters of the thermal decomposition of SS, $[(SS)_2]I^+.I_3^-$, [(SS)(DDQ)], [(SS)(CHL)] and [(SS)(PA)] CT complexes

SS								
			Parameter					
Method	DTG_{max} (°C)	n	E/kJmol^{-1}	Z/s^{-1}	ΔS/Jmol^{-1}K^{-1}	ΔH/kJmol^{-1}	ΔG/kJmol^{-1}	r
HM	279	1	147	9.89×10	−20.4	142	153	0.9993
CR	279	1	131	2.13×10^{11}	−52.3	126	155	0.9791
$([SS)_2]I^+.I_3^-$								
			Parameter					
Method	DTG_{max} (°C)	n	E/kJmol^{-1}	Z/s^{-1}	ΔS/Jmol^{-1}K^{-1}	ΔH/kJmol^{-1}	ΔG/kJmol^{-1}	r
HM	400	3	74	1.10×10^6	−135	80	150	0.9961
CR	400	3	78	1.50×10^5	−151	75	155	0.9921
[(SS)(DDQ)]								
			Parameter					r
Method	DTG_{max} (°C)	n	E/kJmol^{-1}	Z/s^{-1}	ΔS/Jmol^{-1}K^{-1}	ΔH/kJmol^{-1}	ΔG/kJmol^{-1}	
HM	250	2	135	2.70×10^{11}	−30	128	145	0.9977
CR	250	2	127	2.50×10^{10}	−48	137	146	0.9986
[(SS)(CHL)]								
			Parameter					
Method	DTG_{max} (°C)	n	E/kJmol^{-1}	Z/s^{-1}	ΔS/Jmol^{-1}K^{-1}	ΔH/kJmol^{-1}	ΔG/kJmol^{-1}	r
HM	330	2	610	3.00×10^6	−108	100	165	0.9954
CR	330	2	932	3.60×10^5	−140	88	175	0.9965
[(SS)(PA)]								
			Parameter					r
Method	DTG_{max} (°C)	n	E/kJmol^{-1}	Z/s^{-1}	ΔS/Jmol^{-1}K^{-1}	ΔH/kJmol^{-1}	ΔG/kJmol^{-1}	
HM	310	2	60	1.25×10^7	−115	59	98	0.9996
CR	310	2	55	8.57×10^5	−130	52	100	0.9992

n = number of decomposition steps

Horowitz and Metzger (HM) approximation method[31]

These authors derived the relation

$$\ln[-\ln(1-\alpha)] = \frac{E}{RT_m}\Theta \tag{8}$$

where α, is the fraction of the sample decomposed at time t and $\Theta = T - T_m$.

A plot of $\ln[-\ln(1-\alpha)]$ against Θ, was found to be linear (Figure 8) from the slope of which E, was calculated and Z can be deduced from the relation

$$Z = \frac{E\varphi}{RT_m^2}\exp\left(\frac{E}{RT_m}\right) \tag{9}$$

where φ is the linear heating rate and the order of reaction, n, can be calculated from the relation in Equation (10)

$$n = 33.64758 - 182.295\alpha_m + 435.9073\alpha_m^2 - 551.157\alpha_m^3 + 357.3703\alpha_m^4 - 93.4828\alpha_m^5 \tag{10}$$

where α_m is the fraction of the substance decomposed at T_m.

Coats and Redfern (CR) integral method[32]

For first-order reactions, the Coats-Redfern equation may be written in the form

$$\ln\left[\frac{-\ln(1-\alpha)}{T^2}\right] = \ln\left(\frac{ZR}{\varphi E}\right) - \frac{E}{RT} \tag{11}$$

A plot of $\ln\left[\frac{-\ln(1-\alpha)}{T^2}\right]$ against $1/T$ was found to be linear (Figure 8) from the slope of which E, was calculated and Z can be deduced from the intercept. The enthalpy of activation, ΔH, and the free enthalpy of activation, ΔG, can be calculated via Equation (12).

$$\Delta H = E - RT_m;\ \Delta G = \Delta H - T_m\Delta S \tag{12}$$

The kinetic parameters were evaluated using two of the above-mentioned methods by graphical means and are listed in Table 8. The satisfactory values of correlation coefficients (~1) in all cases indicates good agreement with experimented data and the values of kinetic parameters are reasonable and in good agreement.

References

[1] L. Sutherland, D. Roth, P. Beck, G. May, K. Makiyama, *Cochrane Database Syst. Rev.* **2000**, CD000543.
[2] S. B. Hanauer, W. J. Sandborn, A. Kornbluth, S. Katz, M. Safdi, S. Woogen, G. Regalli, C. Yeh, N. Smith-Hall, F. Ajayi, *Am. J. Gastroenterol.* **2005**, *100*, 2478.
[3] C. M. Bell, F. M. Habal, *Am. J. Gastroenterol.* **2007**, *92*, 2201.
[4] O. Diav–Citrin, Y. H. Park, G. Veerasuntharam, H. Polachek, M. Bologa, A. Pastuszak, G. Koren, *Gastroenterology* **1998**, *114*, 23.
[5] D. K. Roy, A. Saha, A. K. Mukherjee, *Spectochim. Acta A* **2005**, *61*, 2017.
[6] M. M. A. Hamed, M. I. Abdel-Hamid, M. R. Mahmoud, *Monatsh. Chem.* **1998**, *129*, 121.
[7] A. Dozal, H. Keyzer, H. K. Kim, W. W. Way, *Int. J. Antimicrob. Agent* **2000**, *14*, 261.
[8] R.S. Mulliken, *J. Am. Chem. Soc.* **1950**, *72*, 600.
[9] R. S. Mulliken, *J. Am. Chem. Soc.* **1952**, *74*, 811.
[10] M. S. Refat, L. A. El-Zayat, O. Z. Yeşilel *Spectrochim. Acta Part A* **2010**, *75*, 745.
[11] M. Pandeeswaran, K. P. Elango *Spectrochim. Acta Part A* **2009**, *72*, 789.
[12] A. S. Al-Attas, M. M. Habeeb, D. S. Al-Raimi, *J. Mol. Liquid.* **2009**, *148*, 58.
[13] S.-Ro Lee, M. M. Rahman, K. Sawada, M. Ishida, *Biosensors and Bioelectronics* **2009**, *24*, 1877.
[14] D. A. Skoog, *Principle of Instrumental Analysis*, 3rd edn., Saunders College Publishing: New York, USA, **1985**, Ch. 7.
[15] W. Kiefer, H. J. Bernstein, *Chem. Phys. Lett.* **1972**, *16*, 5.
[16] L. Andrews, E. S. Prochaska, A. Loewenschuss, *Inorg. Chem.* **1980**, *19*, 463.
[17] K. Kaya, N. Mikami, Y. Udagawa, M. Ito, *Chem. Phys. Lett.* **1972**, *16*, 151.
[18] R. Abu-Eittah, F. Al-Sugeir, *Can. J. Chem.* **1976**, *54*, 3705.
[19] H. Tsubomura, R. P. Lang, *J. Am. Chem. Soc.* **1964**, *86*, 3930.
[20] M. M. Ayad, *Spectrochim. Acta Part A* **1994**, *50*(4), 671.
[21] S. M. Teleb, M. S. Refat, *Spectrochimica Acta Part A* **2004**, *60*(7), 1579.
[22] E. M. Nour, S. M. Teleb, M. A. F. El-Mosallamy, M. S. Refat, *South Afr. J. Chem.* **2003**, *56*.
[23] R. Rathone, S. V. Lindeman, J. K. Kochi, *J. Am. Chem. Soc.* **1997**, *119*, 9393.
[24] G. Aloisi, S. Pignataro, *J. Chem. Soc. Faraday Trans.* **1972**, *69*, 534.
[25] G. Briegleb, *Z. Angew. Chem.* **1964**, *76*, 326.
[26] G. Briegleb, J. Czekalla, *Z. Physikchem. (Frankfurt)* **1960**, *24*, 237.
[27] A. N. Martin, J. Swarbrick, A. Cammarata, *Physical Pharmacy*, 3rd edition. Lee and Febiger: Philadelphia, PA, **1969**, p. 344.
[28] L. J. Bellamy, *The Infrared Spectra of Complex Molecules*, Chapman & Hall: London, **1975**.
[29] R. D. Kross, V. A. Fassel, *J. Am. Chem. Soc.* **1957**, *79*, 38.
[30] E. S. Freeman, B. Carroll, *J. Phys. Chem.* **1958**, *62*, 91.
[31] H. H. Horowitz, G. Metzger, *Anal. Chem.* **1963**, *35*, 1464.
[32] A. W. Coats, J. P. Redfern, *Nature* **1964**, *201*, 68.